

Critical layer thickness for self-assembled InAs islands on GaAs

D. Leonard, K. Pond, and P. M. Petroff

Materials Department, University of California, Santa Barbara, California 93106

(Received 12 May 1994)

Using atomic force microscopy (AFM), we have directly observed the progression of surface morphology of InAs deposited by molecular-beam epitaxy on GaAs(100). InAs self-assembled dots (coherent) or relaxed InAs islands (incoherent) are formed depending on the InAs coverage. The InAs coverage was varied continuously and AFM was used to monitor in detail the nucleation and resulting size and shape transition of the InAs self-assembled dots. Dots of uniform size were observed only at the initial stages of this Stranski-Krastanow growth-mode transition. The self-assembled dot density increased very abruptly with total deposited amount of InAs. Treating this InAs growth-mode transition as a first-order phase transition with InAs total coverage as the critical parameter, we extract a critical thickness for surface elastic relaxation of 1.50 ML.

I. INTRODUCTION

The use of alternating epitaxial layers of material to produce band-gap modulations has generally been restricted to combinations of materials with similar crystal structure and lattice spacing. Defects such as dislocations generated by lattice-mismatch strain are primarily responsible for this restriction. We have reported on a method to exploit lattice mismatch in the $\text{In}_x\text{Ga}_{1-x}\text{As}/\text{GaAs}$ system and achieve three-dimensional potential confinement.¹ This was accomplished by terminating the deposition of highly strained $\text{In}_x\text{Ga}_{1-x}\text{As}$ on GaAs immediately upon the Stranski-Krastanow growth mode transition.² The resulting self-assembled ~ 20 -nm islands of $\text{In}_x\text{Ga}_{1-x}\text{As}$ which form atop a two-dimensional wetting layer were coherently strained and very uniform.³ The lattice-mismatch strain relaxation of $\text{In}_x\text{Ga}_{1-x}\text{As}$ and InAs on GaAs has long been studied,⁴ but the emphasis has generally been on two-dimensional strained layers with dislocation introduction as the only means of strain relaxation. Recently some theoretical considerations of pseudomorphically strained islands have been published.⁵ Furthermore, Drucker extended the approach of Chakraverty⁶ to predict under certain assumptions that a monodisperse island size could be achieved.⁷ General agreement has been obtained with these predictions, but it is still unclear what ultimate limitations exist to obtaining perfectly uniform size distributions. Deviations from the hemispherical island shape assumed in this model have been observed,⁸ requiring a more exact treatment of pseudomorphic island growth for this system. Also, discrepancies exist in reported values of the critical thickness required to induce this relaxation from two to three dimensional growth. These emphasize the need for conclusive information about the nature of this elastic Stranski-Krastanow relaxation for the InAs on GaAs system. Specifically, the nucleation and growth behavior of these islands with varying strain will be of critical importance in complete theoretical modeling of this transition.

In this paper we present atomic force microscopy

(AFM) images of the initial stages of formation of self-assembled dots (SAD's) during InAs deposition upon GaAs. General structural and optical features of SAD's, including signatures of quantum confinement, were presented earlier.⁹ Here we report on the nucleation of SAD and its specific dependence on strain in this system. The total amount of deposited InAs and the nature of monolayer (ML) steps at the surface are shown to be critical growth parameters. In addition to providing insight into the coherent strain relaxation process, the present study suggests an approach to attaining the most uniform SAD's.

II. EXPERIMENTAL DETAILS

Samples studied here were grown by molecular-beam epitaxy (MBE) by depositing InAs directly on a $0.5 \mu\text{m}$ (100) GaAs buffer layer including a GaAs/AlAs ($2 \times 2 \text{ nm}^2$) short-period superlattice, unless otherwise specified. The substrate temperature during InAs deposition was 530°C according to a pyrometer. At this temperature the $c(4 \times 4)$ GaAs reconstruction begins to give way to the (2×4) reconstruction. Above this temperature In significantly desorbs from the surface. A variation in the deposited In coverage was implemented in samples A and C by continuously sweeping a Ta shadow mask across the wafer during InAs deposition. The shadow mask was located ~ 4 mm from the growing surface, allowing As stable surface conditions under the masked portion of the substrate. The As-rich reconstruction was verified by reflection high-energy electron diffraction (RHEED). The InAs coverage sweep produced with this method was 1–4 ML for sample A and 1–3 ML for sample C. Variations in InAs coverage of samples B and D were obtained from nonuniformities of the In flux due to the source geometry in the Varian Gen II MBE machine used. Substrate rotation was not used during InAs deposition in samples B and D, except for the buffer layers. Under a constant As_4 beam equivalent pressure of 7×10^{-6} Torr, cycles of In were deposited corresponding to an average growth rate of 0.01 ML per second. In this way we emu-

late equilibrium surface conditions as closely as possible.

The In flux was calibrated with RHEED oscillations at 530°C by subtracting the Ga flux from the In+Ga flux. After formation of SAD, samples were rapidly cooled to 350°C and removed from the growth chamber. Samples were stored in a vacuum desiccator less than one day before AFM measurements were completed in ambient conditions. This produces a thin oxide layer which does not significantly effect AFM measurement in the range of interest. A SiN tip from a Nanoscope III AFM with a 200- μm cantilever was kept in direct contact with the sample surface for measurement. The AFM height data were calibrated using standard gold gratings and monolayer-height steps (0.30 nm) that were observable on the InAs surface of our samples. AFM images shown here were flattened and planefit with the Nanoscope III software.

III. RESULTS AND DISCUSSION

Figure 1 shows a series of $1 \times 1 \mu\text{m}^2$ AFM images obtained from sample A, where the InAs coverage is swept from approximately 1–4 ML. Images are representative of morphology changes with InAs coverage, but not taken from evenly spaced areas of this sample. At the first stages of growth, a smooth surface is observed.

Monolayer-height steps indicate a slight 0.21° tilt of the substrate toward the (111)A direction. At this InAs coverage, the surface consists of large terraces with an average spacing of 77 ± 35 nm. Such uniform terraces suggest that under these conditions InAs layer growth occurs by movement of In adatoms toward step edges, a fact consistent with large In diffusion lengths which have been reported.¹⁰ The surface normal of this sample slightly exceeds the manufacturer specified limits ($\pm 0.1^\circ$) for nominally flat (100) wafers. AFM thus represent a simple, reliable method for verifying orientations of nearly flat wafers. Small features near terrace edges of 0.5–2 nm in height may be subcritical nuclei for the formation of SAD's.

Intermediate InAs coverage near 1.7 ML produces only SAD's, as in Figs. 1(b) and 1(c). These SAD's are pseudomorphic and defect free as ascertained by earlier TEM studies.¹ A slight reduction in the average size of the islands is associated with the increase in density of SAD with coverage. This dependence of SAD size and shape on increasing InAs coverage will be discussed in detail in the following paragraphs. Figure 1 shows that the most uniform SAD sizes are observed only at the very initial stages of their formation at approximately 1.6 ML.

These SAD's are distinguished from relaxed InAs islands. If InAs growth is continued to coverage well

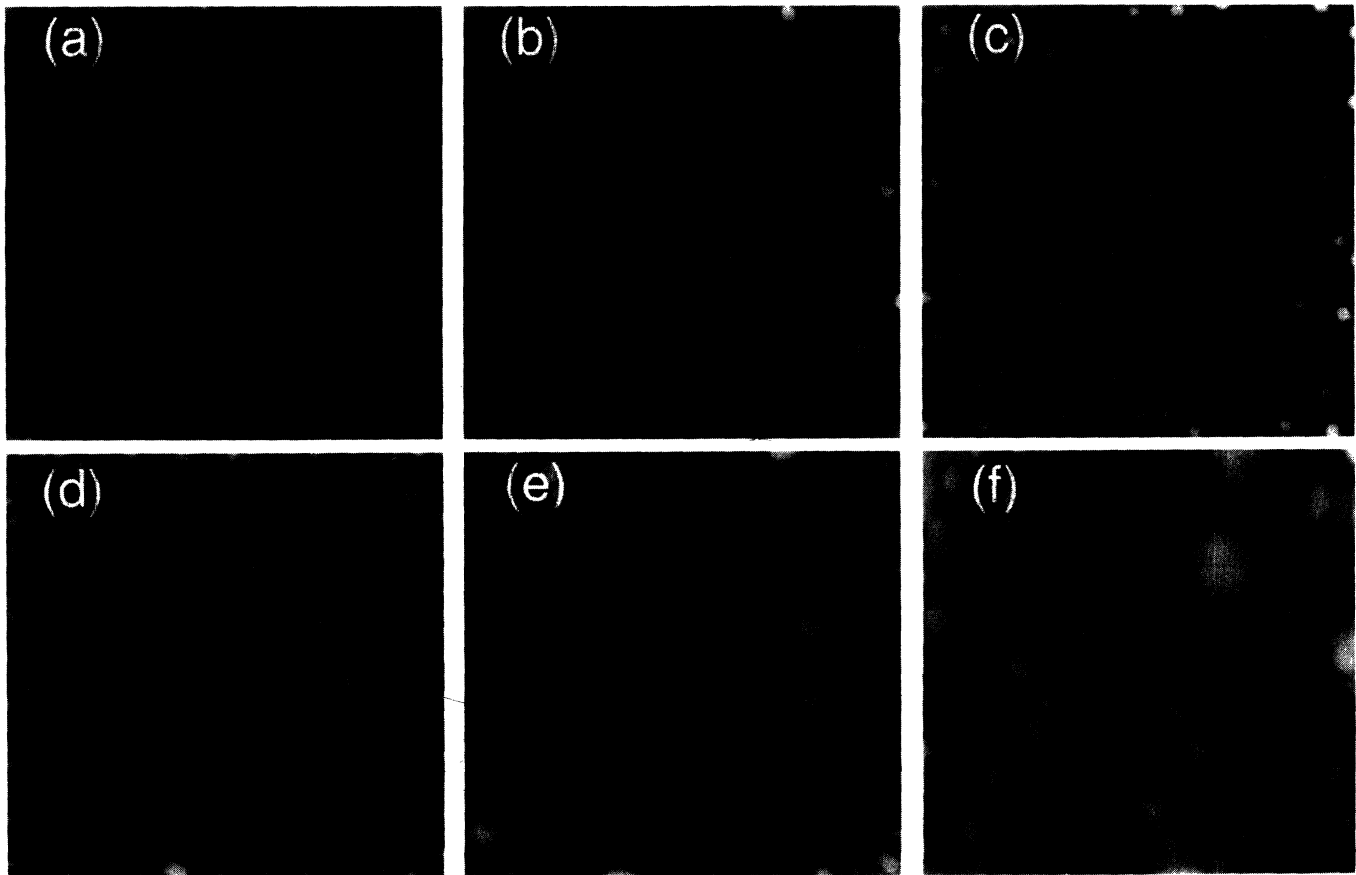


FIG. 1. A series of $1 \times 1 \mu\text{m}^2$ atomic force microscopy images of a range of coverages of InAs on (100) GaAs, from one monolayer in (a) up to four monolayers in (f), produced by use of a Ta shadow mask. The best size uniformity ($\pm 10\%$ in height, $\pm 7\%$ in diameter) of self-assembled islands of InAs is found only at the initial stages of their formation.

beyond 2 ML, dislocated islands will form, as verified in TEM and reported elsewhere.¹¹ It is unclear whether these incoherent islands [Figs. 1(d)–1(f)] are formed by aggregation or coalescence of several SAD's or by growth of a single SAD after introduction of dislocations. Nevertheless it is clear that once formed these incoherent islands grow in size without restriction. This is qualitatively consistent with the model of Drucker discussed earlier, which predicts an accelerated growth rate for relaxed islands. Growth of these larger islands is concurrent with the dissolution of the SAD, indicating that relaxed islands act as sinks for surface mobile cations.¹² The mass transport of In adatoms from the SAD's into relaxed islands indicates a dynamic growing surface, with a large cation surface mobility and a high rate of adatom attachment and detachment to islands. The shape of a relaxed island resembles that of roughness observed with optical microscopy on thick InAs epitaxial layers. It is the relaxed islands which then coalesce to produce a continuous thick film.

The dependence of InAs island density and diameter on growth parameters such as substrate temperature and As flux have been documented.¹³ However, we have found that the most significant changes in SAD's are associated with the total InAs coverage. In particular, for sample A the density of the SAD abruptly increases to a value of $1 \times 10^{10} \text{ cm}^{-2}$ between the regions imaged by Figs. 1(a) and 1(c), separated by only 1 mm on the wafer. We therefore deduce that the strain, induced by increasing the total amount of deposited InAs, is a more critical growth parameter for the tuning of SAD size and density. To ascertain the exact coverage dependence of SAD density, as well as other structural variations, an additional type of sample was grown. On sample B, changes in SAD's were produced across a 2-in. wafer by the InAs flux variations from the In effusion cell. Figure 2 shows a series of $5 \times 5 \mu\text{m}^2$ AFM images obtained from sequential areas of this sample. Measured areas were spaced by 0.7 mm on the 2-in. wafer, with the sample imaged in Fig. 2(c) being in closest proximity to the In effusion cell. Using well-known predictions of the flux variations¹⁴ for our source-sample geometry, we estimate that 0.7 mm represents only a 0.01-ML change in the amount of deposited InAs. The SAD density increases monotonically from 8×10^6 to $2.5 \times 10^8 \text{ cm}^{-2}$ with increased coverage of only 0.021 ML. Proper control of the SAD density would thus require growth rate accuracy within at least ± 0.021 ML. The increasing numbers of SAD allow greater relief of the strain which increases with further InAs coverage. These observations indicate that the most important parameter for the tuning of the SAD density is the InAs coverage.

In Fig. 3 we plot the SAD density versus the estimated total InAs coverage on sample B. For this plot we obtained extensive data in the coverage range of 1.6 ML, corresponding to a SAD density of $\approx 1 \times 10^9 \text{ cm}^{-2}$. Below this coverage the low probability of measuring a single SAD causes less precise determination of the density. The SAD density is essentially zero until a certain critical coverage, at which the value increases sharply. The data are fit with a function of the form

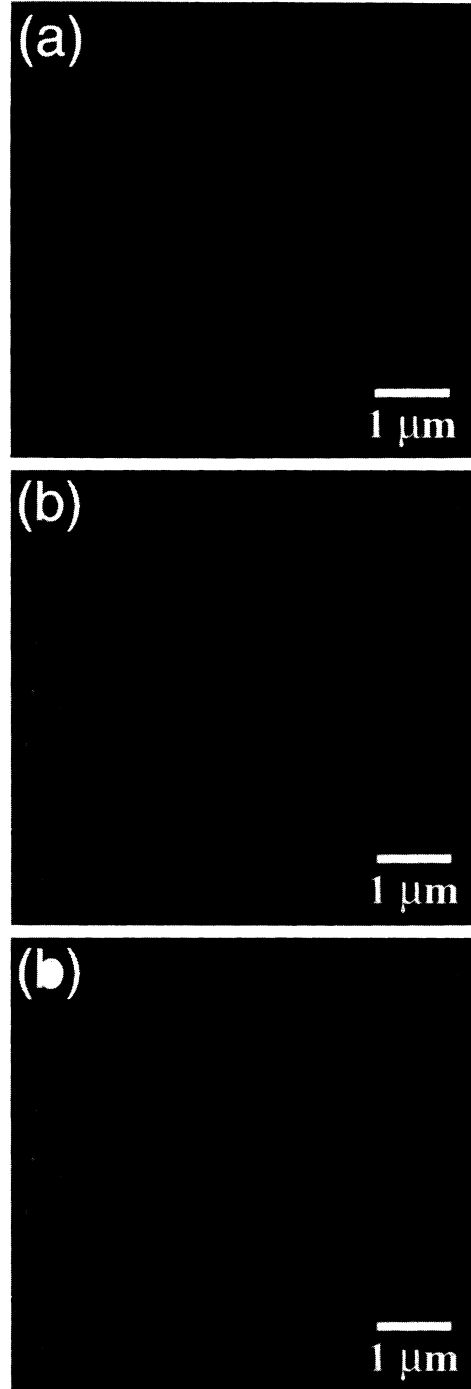


FIG. 2. A series of $5 \times 5 \mu\text{m}^2$ atomic force microscopy images of a range in densities of self-assembled dots of InAs on GaAs. The sample areas imaged in (a) through (c) were separated by 1 mm on a 2-in wafer, which was not rotated during deposition of InAs. Images are in the order of decreasing distance from the In effusion cell.

$$\rho_{\text{SAD}} = \rho_0 (\Theta - \Theta_c)^\alpha .$$

In this case ρ_{SAD} is the SAD density, and Θ is the estimated InAs coverage. This functional behavior is that

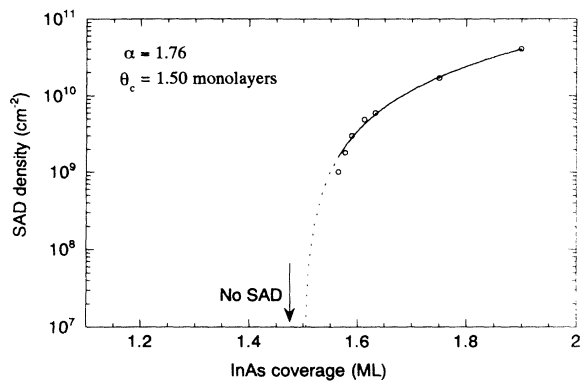


FIG. 3. Density of self-assembled dots vs InAs coverage. Treating these data as a first-order phase transition gives a critical thickness of 1.50 monolayers.

of a first-order phase transition, with SAD density representing an order parameter. The critical coverage θ_c , the exponent α , and the normalization density ρ_0 were obtained from a least-squares fit shown by the solid line. From the best fit to the data, we extract a ρ_0 of $2 \times 10^{11} \text{ cm}^{-2}$, an exponent of $\alpha = 1.76$, and a critical InAs coverage of 1.50 ML. Because of the high sensitivity of AFM, we are able to observe the initial response of the surface to increasing mismatch strain in the InAs epitaxial layer. Consequently, we report a value of the criti-

cal thickness lower than expected.

A statistical analysis of many such images has been performed with the use of a computer program which records diameter and height of SAD from AFM images. Histograms of the SAD height and diameter are created from several nearby $1 \times 1 \mu\text{m}^2$ AFM images from samples B and C, corresponding to the estimated coverage of 1.6, 1.65, 1.75 and 1.9 ML for Figs. 4(a)–4(d), respectively. A typical AFM image for each coverage is also shown. SAD size uniformity, reported as standard deviation in AFM data, of $\pm 10\%$ in height and $\pm 7\%$ in diameter was observed at the initial stages of formation. This uniformity degraded for InAs coverage higher than that shown in Fig. 4(a). The mean diameter decreased from nearly 30 nm to below 20 nm at higher InAs coverage. The additional strain induced by further coverage with InAs evidently causes no further increase in the diameter or height of SAD. Instead, the SAD form at a certain size ($\approx 30\text{-nm}$ diameter) after which only an increase in the nucleated density of SAD takes place. It is likely that the greater amount of nucleation leads to the SAD size reduction through In surface diffusion away from already formed SAD. At a density of approximately $4 \times 10^{10} \text{ cm}^{-2}$, large relaxed InAs islands form, and the SAD density does not increase further.

It is rather unexpected that after the initial nucleation, further InAs coverage produces not larger SAD, but increasing numbers of SAD. This suggests an energy bar-

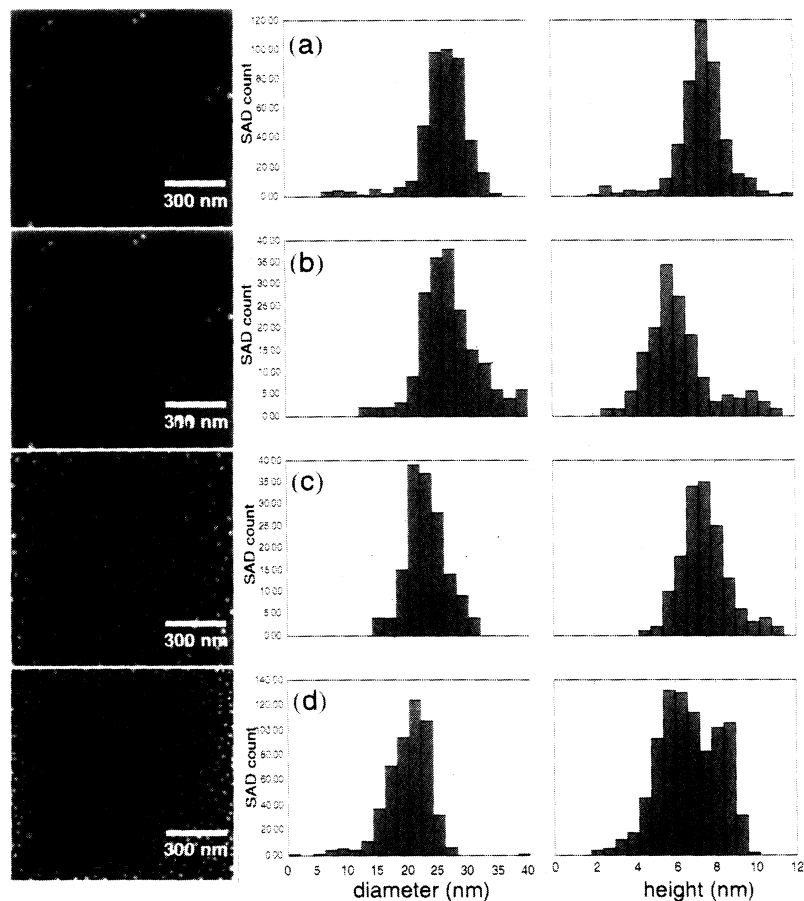


FIG. 4. A series of $1 \times 1 \mu\text{m}^2$ atomic force microscopy images of self-assembled InAs islands formed with varying coverages of InAs on GaAs. Estimated InAs coverage is 1.6, 1.65, 1.75, and 1.9 for (a) through (d), respectively. Distributions of diameter and height shown next to these typical images were measured from several images from nearby $1 \times 1 \mu\text{m}^2$ areas.

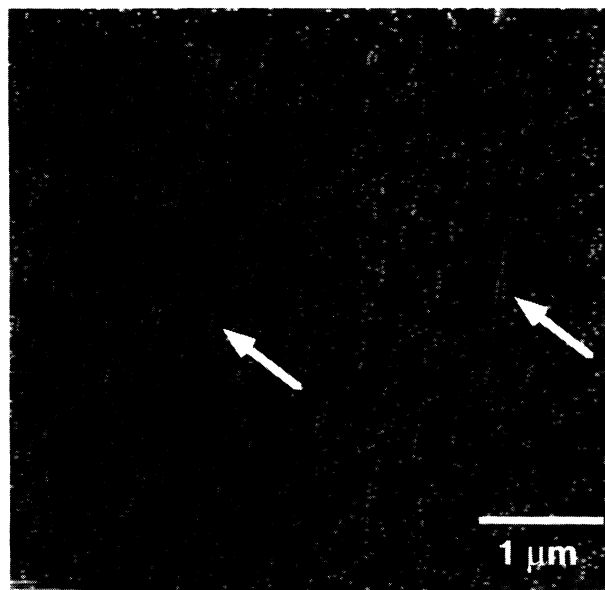


FIG. 5. A $5 \times 5 \mu\text{m}^2$ image of self-assembled dots grown on GaAs without an AlAs (2 nm) \times GaAs (2 nm) short-period superlattice. Arrows show dots preferentially nucleating at surface features.

rier to SAD growth. This energy barrier to continued SAD growth may simply be the energy barrier for the nucleation of a misfit dislocation.⁷ Additionally, a strong correlation must exist between SAD formation and the nature of nucleation of the starting surface. The selection of nucleation sites by SAD can be observed directly by AFM. In Figs. 1(a)–1(c), monolayer steps were observed that indicated preferential SAD nucleation at step edges. It is unknown if the initial nucleation [Fig. 1(b)] occurs at kinks into the step edge or if the initial nucleation process causes depletion of the nearby terrace. In any case these images indicate that surface steps play a large role in determining SAD nucleation, and therefore a large role in determining SAD structural properties.

This is further illustrated in Fig. 5, which shows AFM images from sample D. Sample D was identical to sample B, but grown without the usual short-period superlattice as part of the GaAs buffer layer. This led to a gradual corrugation of the surface with a period of $\approx 0.5 \mu\text{m}$ along a (110) direction. At surface positions where several steps are clustered, indicated by arrows in Fig. 5, SAD's become linearly ordered along the step. Exploitation of this behavior could make lateral organization of SAD's possible. Regular arrays of steps or surface features with the proper spacing would be required. Growth on off-axis substrates could create such an array, but with a lateral pitch generally smaller than the size of the SAD (35 nm for a 0.5° tilt). Referring to Fig. 2, SAD area densities in the range of $8 \times 10^6 \text{ cm}^{-2}$ are achievable on portions of the wafer and with a suitable growth interruption. This places the density of the SAD within the spatial limits of common lithography, and opens the possibility so isolating single SAD's for electronic devices.

From AFM height and diameter data for SAD's, we

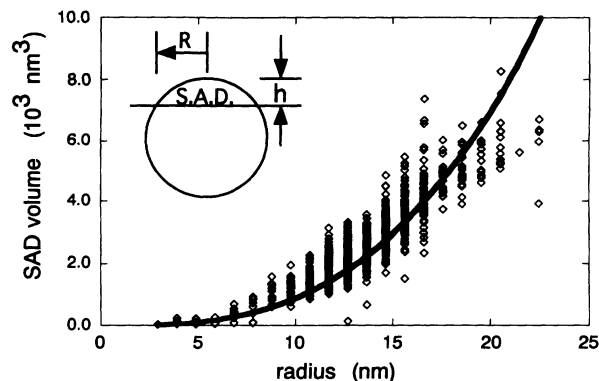


FIG. 6. Volume of individual InAs self-assembled dots vs radius as measured from AFM. The data are fit with a volume equation derived by assuming the inset shape.

have directly recorded the SAD volume. In Fig. 6 we plotted the volume of individual SAD's versus the in-plane radius for all SAD's measured to data. From AFM data the SAD's are found to be radially symmetric and planoconvex, similar to a lens. An object of similar shape formed by the intersection of a sphere and a plane is assumed, drawn schematically in the inset of Fig. 6. The volume of such an object can be estimated by the equation

$$V = (\pi/6)[(1/Q^3) + (3/Q)]R^3,$$

where R is the SAD radius and Q is the aspect ratio of the SAD radius and height. The least-squares fit of the data in Fig. 6 with this equation gives an average aspect ratio $Q \approx 2$. Negative and positive deviations from this curve fit correspond to deviations from the assumed shape toward higher and lower Q , respectively. For larger measured radii consistent deviations indicate that Q may be larger, although the data are fit quite well with a constant Q of 2. Moisson *et al.* have reported SAD aspect ratios independent of SAD size,⁸ which is qualitatively consistent with our results. However, they found that Q was a factor of ≈ 2 larger than here. Repeated calibration of AFM height measurement with both Au standards and with monolayer-height steps on the samples ensures the correctness of our reported values. Differences could perhaps be attributed to variations in SAD growth conditions or different surface oxidation rates.

The SAD density increase with InAs coverage causes the total number of In atoms included in the SAD to increase from 9.72×10^{13} In atoms/ cm^{-2} to 2.29×10^{14} In atoms per cm^{-2} . These In atoms cannot be accounted for by the newly deposited amount equivalent to only 2.52×10^{13} atoms. Thus with increasing SAD density, more of the InAs previously deposited on the substrate is incorporated into SAD. This can only take place with a corresponding decrease in the thickness of the two-dimensional Stranski-Krastanow wetting layer, involving surface mass transport of In.

IV. CONCLUSIONS

We have used AFM to observe the density, size, and shape transition of InAs self-assembled dots with increasing InAs deposition on GaAs. SAD's are observed directly by AFM to nucleate at monolayer terrace edges and larger features on the sample surface, suggesting the possibility of controllably ordering these SAD's. The size uniformity of SAD's was $\pm 10\%$ in height and $\pm 7\%$ in diameter only at the initial stages of the Stranski-Krastanow growth mode transition. The formation of SAD's was found to depend critically on the total InAs coverage. It was shown that the size and volume change of the SAD's involves In atoms from the two-dimensional wetting layer. SAD density was sensitive to 0.01 ML of InAs, well within the error of common growth rate mea-

surements. Treating this system as a first-order phase transition with InAs total coverage as the critical parameter, we extract a critical thickness for elastic relaxation of 1.50 ML.

ACKNOWLEDGMENTS

We would like to thank the Materials Research Laboratory (DMR No. 9123048), and acknowledge financial support from the National Science Foundation Center for Quantized Electronic Structures (DMR No. 91-20007) and the Air Force Office of Scientific Research (F9620-98-J0214). We thank Axel Lorke and John English for their assistance in design of the Ta shadow mask. D.L. would like to thank Mohan Krishnamurthy for motivating this work.

-
- ¹D. Leonard, M. Krishnamurthy, C. M. Reaves, S. P. DenBaars, and P. M. Petroff, *Appl. Phys. Lett.* **63**, 3203 (1993).
- ²I. N. Stranski and L. Von Krastanow, *Akad. Wiss. Lit. Mainz Abh. Math. Naturwiss. Kl. IIB* **146**, 797 (1939).
- ³D. Leonard, M. Krishnamurthy, C. M. Reaves, S. P. DenBaars, and P. M. Petroff, *Appl. Phys. Lett.* **63**, 3203 (1993), and references therein. See also J. M. Moisson, F. Houzay, F. Barthe, L. Leprince, E. Andre, and O. Vatel, *ibid.* **64**, 196 (1994).
- ⁴See, for example, K. L. Kavanagh, J. C. P. Chang, J. Chen, J. M. Fernandez, and H. H. Wieder, *J. Vac. Sci. Technol. B* **10**, 1820 (1992); Z. Lilientalweber, Y. Chen, P. Werner, N. Zakharov, W. Swider, and J. Washburn, *ibid.* **11**, 1379 (1993); S. M. Lord, B. Pezeshki, and J. S. Harris, Jr., *Electron. Lett.* **28**, 1193 (1992).
- ⁵J. Drucker, *Phys. Rev. B* **48**, 18 203 (1993); J. Tersoff, *Appl. Phys. Lett.* **62**, 693 (1993).
- ⁶B. K. Chakraverty, *J. Phys. Chem. Solids* **28**, 2401 (1967); **28**, 2413 (1967).
- ⁷J. Drucker, *Phys. Rev. B* **48**, 18 203 (1993).
- ⁸J. M. Moisson, F. Houzay, F. Barthe, L. Leprince, E. Andre, and O. Vatel, *Appl. Phys. Lett.* **64**, 196 (1994); see also Ref. 1.
- ⁹H. Drexler, D. Leonard, W. Hansen, J. P. Kotthaus, and P. M. Petroff (unpublished); D. Leonard, S. Fafard, K. Pond, Y. H. Zhang, J. L. Merz, and P. M. Petroff, in *Proceedings of the Conferences on Physics and Chemistry and Surfaces and Interfaces*, Mohonk, NY, 1994 [*J. Vac. Sci. Technol. B* (to be published)]; G. Wang, S. Fafard, D. Leonard, J. E. Bowers, J. L. Merz, and P. M. Petroff, *Appl. Phys. Lett.* **64**, 2815 (1994).
- ¹⁰H. Toyoshima, T. Shitara, P. N. Fawcett, J. Zhang, J. H. Neave, and B. A. Joyce, *J. Appl. Phys.* **73**, 2333 (1993), and references therein.
- ¹¹S. Guha, A. Madhukar, and K. C. Rajkumar, *Appl. Phys. Lett.* **57**, 2110 (1990).
- ¹²M. Krishnamurthy, J. Drucker, and J. A. Venables, *J. Appl. Phys.* **69**, 6461 (1991).
- ¹³D. Leonard, M. Krishnamurthy, S. Fafard, J. L. Merz, and P. M. Petroff, *J. Vac. Sci. Technol. B* **12**, 1063 (1994); P. Chen *et al.*, in *Proceedings of the Conference on Physics and Chemistry of Surfaces and Interfaces*, Mohonk, NY, 1994 (Ref. 9).
- ¹⁴D. A. Herman and H. Sitter, *Molecular Beam Epitaxy* (Springer-Verlag, Berlin, 1989).

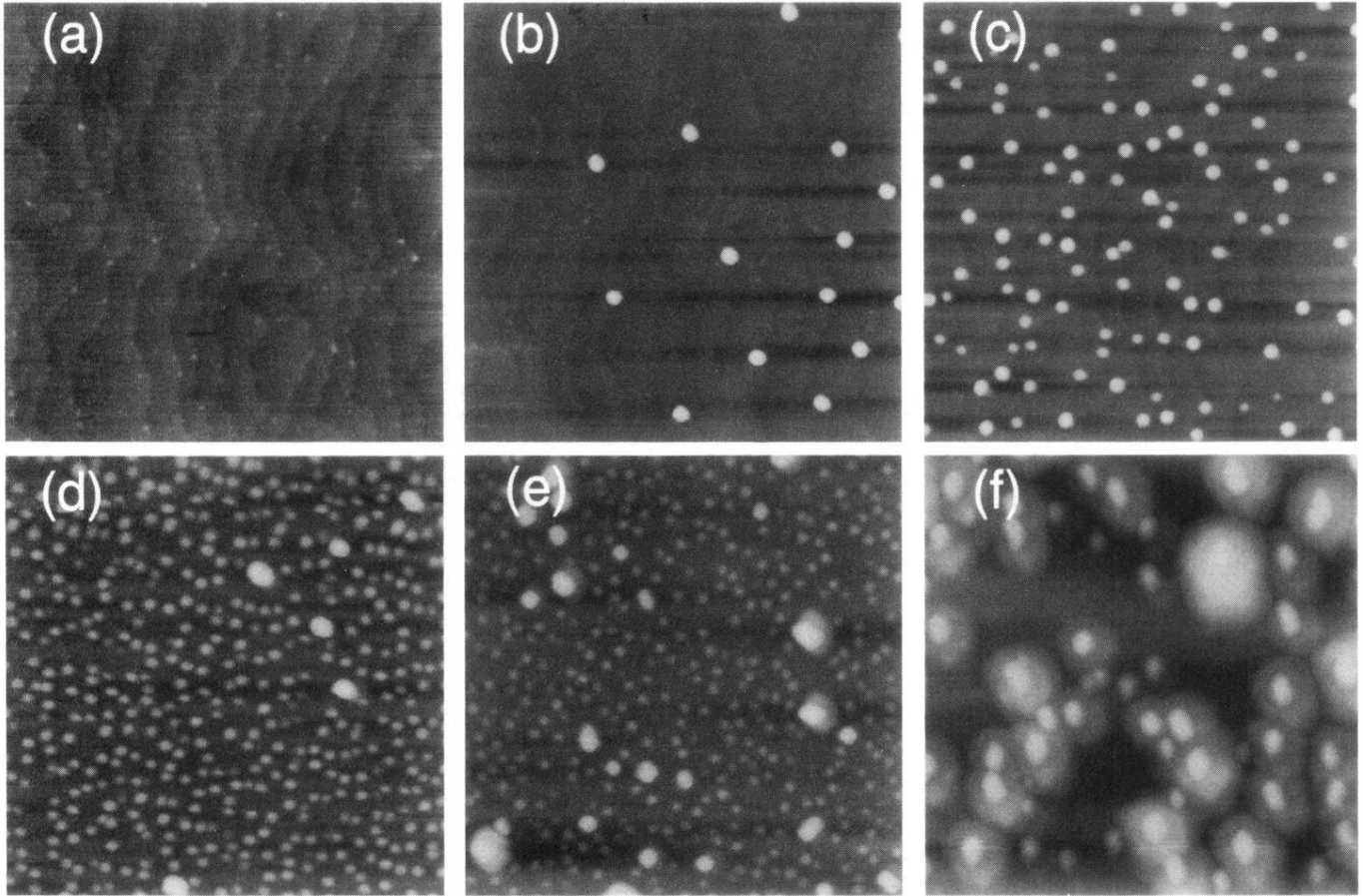


FIG. 1. A series of $1 \times 1 \mu\text{m}^2$ atomic force microscopy images of a range of coverages of InAs on (100) GaAs, from one monolayer in (a) up to four monolayers in (f), produced by use of a Ta shadow mask. The best size uniformity ($\pm 10\%$ in height, $\pm 7\%$ in diameter) of self-assembled islands of InAs is found only at the initial stages of their formation.

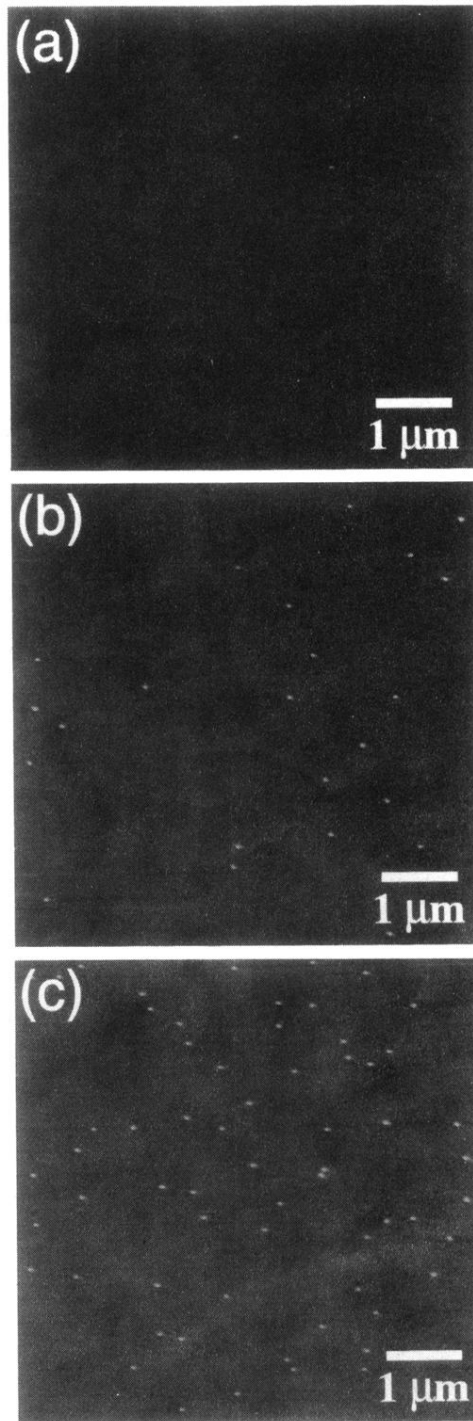


FIG. 2. A series of $5 \times 5 \mu\text{m}^2$ atomic force microscopy images of a range in densities of self-assembled dots of InAs on GaAs. The sample areas imaged in (a) through (c) were separated by 1 mm on a 2-in wafer, which was not rotated during deposition of InAs. Images are in the order of decreasing distance from the In effusion cell.

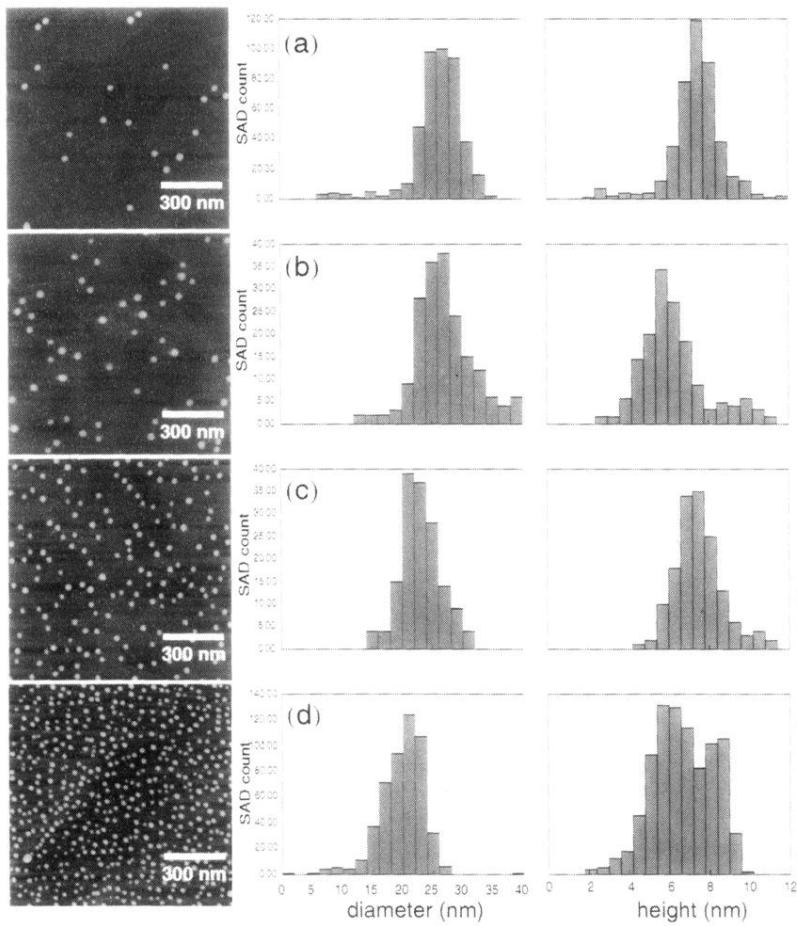


FIG. 4. A series of $1 \times 1 \mu\text{m}^2$ atomic force microscopy images of self-assembled InAs islands formed with varying coverages of InAs on GaAs. Estimated InAs coverage is 1.6, 1.65, 1.75, and 1.9 for (a) through (d), respectively. Distributions of diameter and height shown next to these typical images were measured from several images from nearby $1 \times 1 \mu\text{m}^2$ areas.

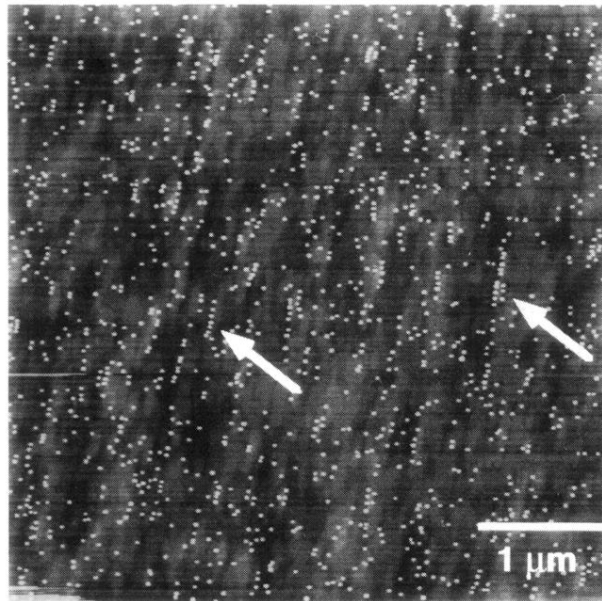


FIG. 5. A $5 \times 5 \mu\text{m}^2$ image of self-assembled dots grown on GaAs without an AlAs (2 nm) \times GaAs (2 nm) short-period superlattice. Arrows show dots preferentially nucleating at surface features.